Measurement of cosmic rays with LOFAR

2016 J. Phys.: Conf. Ser. 718 052035

(http://iopscience.iop.org/1742-6596/718/5/052035)

XIV International Conference on Topics in Astroparticle and Underground Physics (TAUP 2015) IOP Publishing
Journal of Physics: Conference Series **718** (2016) 052035 doi:10.1088/1742-6596/718/5/052035

Measurement of cosmic rays with LOFAR

L Rossetto[1], S Buitink[2], A Corstanje[1], J E Enriquez[1], H Falcke[1,3,4], J R Hörandel[1,3], A Nelles[5], J P Rachen[1], P Schellart[1], O Scholten[6,7], S ter Veen[1,4], S Thoudam[8] and T N G Trinh[6]

[1] Department of Astrophysics / IMAPP, Radboud University Nijmegen, P.O. Box 9010, 6500 GL, Nijmegen, The Netherlands
[2] Astrophysical Institute, Vrije Universiteit Brussel, Pleinlaan 2, 1050 Brussels, Belgium
[3] NIKHEF, Science Park Amsterdam, 1098 XG, Amsterdam, The Netherlands
[4] Netherlands Institute of Radio Astronomy (ASTRON), Postbus 2, 7990 AA Dwingeloo, The Netherlands
[5] Department of Physics and Astronomy, University of California Irvine, Irvine, CA 92697-4575, USA
[6] KVI-CART, University Groningen, P.O. Box 72, 9700 AB, Groningen, The Netherlands
[7] Interuniversity Institute for High-Energy, Vrije Universiteit Brussel, Pleinlaan 2, 1050 Brussels, Belgium
[8] Department of Physics and Electrical Engineering, Linnéuniversitetet, 35195 Växjö, Sweden

E-mail: l.rossetto@astro.ru.nl

Abstract. The LOw Frequency ARay (LOFAR) is a multipurpose radio-antenna array aimed to detect radio signals in the $10 - 240$ MHz frequency range, covering a large surface in Northern Europe with a higher density in the Northern Netherlands. Radio emission in the atmosphere is produced by cosmic-ray induced air showers through the interaction of charged particles with the Earth magnetic field. The detection of radio signals allows to reconstruct several properties of the observed cascade. We review here all important results achieved in the last years. We proved that the radio-signal distribution at ground level is described by a two-dimensional pattern, which is well fitted by a double Gaussian function. The radio-signal arrival time and polarization have been measured, thus providing additional information on the extensive air shower geometry, and on the radio emission processes. We also showed that the radio signal reaches ground in a thin, curved wavefront which is best parametrized by a hyperboloid shape centred around the shower axis. Radio emission has also been studied under thunderstorm conditions and compared to fair weather conditions. Moreover, by using a hybrid reconstruction technique, we performed mass composition measurements in the energy range $10^{17} - 10^{18}$ eV.

1. Introduction

Radio emission from extensive air showers was detected for the first time by Jelley et al. in 1965 [1]. Since 2005 radio experiments like CODALEMA [2] and LOPES [3] have started detecting air showers up to an energy of 10^{18} eV, thus confirming the radio emission mechanisms of cosmic rays in the Earth atmosphere. In the last years, new measurements have been performed with the LOFAR experiment [4], and improvements in the understanding of the radio emission processes of extensive air showers have been made. In the present article, an overview is given about all important achievements obtained by analyzing data detected by LOFAR since 2011. In section 2 results from the antenna calibration campaign are shown together

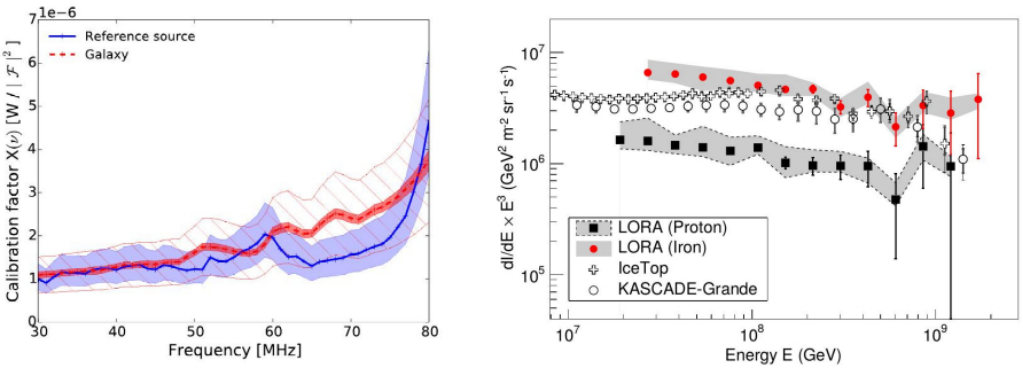

Figure 1. *Left*: calibration factor as function of frequency across the LBA antenna frequency band, as obtained by using a reference source attached from a crane (blue line) and the Galaxy as a reference source (red line). Statistical uncertainties are shown as dark blue and red regions, while systematic uncertainties are illustrated by the blue filled and red dashed area, respectively [5]. *Right*: all-particle cosmic ray spectrum measured with LORA for pure protons (black squares) and iron nuclei (red points). Statistical and systematic uncertainties are represented by bars and shaded areas, respectively [6].

with the energy spectrum obtained from the LORA scintillator array. The characterization of radio emission pattern at ground level and polarization of the radio signal in fair weather and thunderstorm conditions are described in section 3. The study of the particle arrival direction through the evaluation of different wavefront shapes is described in section 4, together with results of the primary particle mass composition analysis. Conclusions and outlook are summarized in section 5.

2. Antenna calibration and energy spectrum

The absolute calibration of LOFAR antennas is one of the key points for air shower measurements. Since radio signals in the atmosphere have a typical width of tens of nanoseconds, it is not possible to use methods based on flux calibration of standard sources, as done in radio astronomical observations. Several campaigns have been conducted at LOFAR in order to acquire an absolute calibration of the LBA antennas which operate in the frequency range $30-80$ MHz. The results of two different studies are shown in figure 1-*left*: the blue line depicts measurements of a calibrated radio source that was suspended from a crane, while the red line represents results obtained by using the Galactic radio emission as a reference source [5]. The two results are in agreement within each others, and with calibration measurements obtained by LOPES and Tunka-Rex experiments as well.

Furthermore, the all-particle energy spectrum of cosmic rays has been measured in the energy range $10^{16} - 10^{18}$ eV [6] by using the LORA particle detector array [7]. Figure 1-*right* shows the obtained energy spectrum by assuming primary protons (black squares) or iron nuclei (red points), together with the results obtained by the IceTop and KASCADE-Grande experiments. This provides an absolute energy scale for cosmic ray measurements at LOFAR.

3. Characterization of cosmic-ray radio emission

Secondary charged particles, produced by the interaction of primary cosmic rays with the atmospheric nuclei, emit radio signals. Radio emission is generated by two mechanisms, the *geomagnetic* and the *charge excess process*, also called *Askaryan effect* [8]. The dominant process is the geomagnetic one in which radio emission is produced by electrons and positrons that are accelerated in opposite directions by the Earth magnetic field $\vec{B}$. As consequence, the generated radio emission is linearly polarized in the direction of the Lorentz force $\vec{v} \times \vec{B}$, where $\vec{v}$ is the

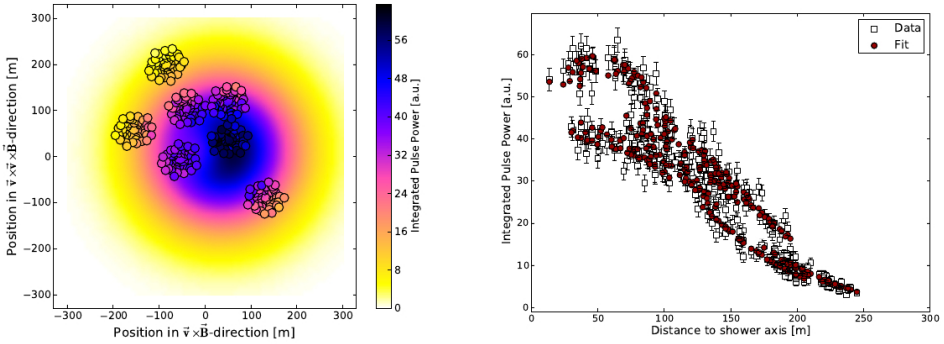

Figure 2. *Left*: integrated radio signal for an air shower in the frequency range between $30-80$ MHz, and projected to the shower plane, as detected by antennas of LOFAR central stations (circles). The coloured background represents the result of the double Gaussian fit. *Right*: integrated radio signal for the same shower as function of distance from the shower axis for data (white squares) and fit (red points) [10].

propagation velocity vector of the shower which is parallel to the shower axis, and $\vec{B}$ represents the direction and strength of the Earth magnetic field. A secondary mechanism is the Askaryan effect which results from a negative charge excess at the shower front. This is created by electrons which are knocked-out by an energy transfer from shower particles to the air molecules, and by a decreasing number of positrons due to annihilation. The generated radio emission is in this case polarized in the radial direction towards the shower axis.

The combination of these two mechanisms creates an asymmetric distribution of the total radio signal in the shower plane, i.e. a plane perpendicular to the shower axis. The lateral distribution of the emitted radio signal has been studied as function of distance from the shower axis, and it has been shown that it is well described by a double Gaussian function. The analysis has been conducted in both the low frequency band $30-80$ MHz [10],[11], and the high frequency band $110-240$ MHz [12], and results have been found to be in agreement. Figure 2-*left* shows the integrated radio signal in the shower plane as detected by each antenna of the LOFAR central stations in the frequency range between $30-80$ MHz. The coloured background shows the results of the fit performed using a double Gaussian function. Figure 2-*right* shows the total radio signal detected by the same stations as function of distance from the shower axis.

Polarization of radio emission has been studied in detail [13]. In figure 3-*left* the polarization footprint for an air shower detected during fair weather conditions is shown in the shower plane. The arrows represent the polarization direction of radio signals detected by each antenna; the polarization direction points along the $\vec{v}\times\vec{B}$ axis which demonstrates that radio emission is mostly dominated by the geomagnetic process. It has also been showed that the contribution of the charge excess effect increases with increasing distance from the shower axis and decreasing zenith angle [13]. The polarization pattern of radio signals has also been studied during thunderstorms. Results exhibit that radio emission is not anymore linearly polarized along the $\vec{v}\times\vec{B}$ direction. Moreover, by using simulations with a simple two-layer model for the atmospheric electric field it was possible to reproduce the characteristics of radio emission during thunderstorms [14],[15].

4. Arrival direction, energy, and mass composition measurements

The shape of the shower front has been studied in order to reconstruct the arrival direction of primary particles with the highest possible precision. Arrival times of the shower wavefront for different air showers have been fitted with conical, spherical, and hyperbolic functions. It was found that the shower wavefront is best parametrized as a hyperboloid, resulting in an accuracy

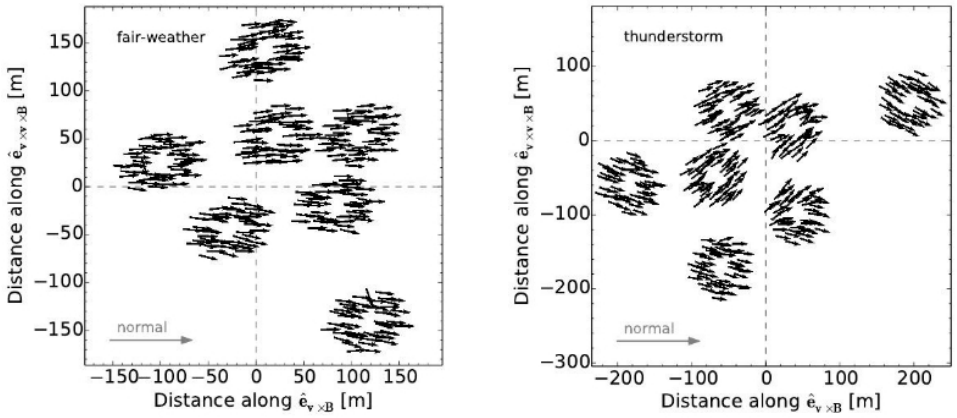

Figure 3. *Left*: polarization footprint on the shower plane for an air shower recorded during fair weather conditions in the frequency range $30-80$ MHz. Each arrow represents the electric field measured by one antenna. The arrows direction are defined by the polarization angle with respect to the $\vec{v}\times\vec{B}$ axis, and the arrows length are proportional to the degree of polarization [13]. *Right*: polarization footprint on the shower plane for an air shower recorded during thunderstorm conditions in the frequency range $30-80$ MHz [14].

of the cosmic ray arrival direction of better than 1° [16]. This allows to reconstruct the core position based on air shower radio measurements in an independent way with respect to the well-established scintillator technique used so far at LOFAR by the LORA array.

As previously described, the distribution of the integrated radio signal at ground level has been parametrized by using a double Gaussian function. The parameters of the fit equation are sensitive to properties of the primary particle. It has been shown that the integral of the measured radio power density is proportional to the energy content of the shower. Results were found to be in agreement with the energy reconstructed by the particle detector array LORA, as well as the energies derived from Monte Carlo simulations. Moreover, it was found that the width of the radio footprint is proportional to the distance of the shower maximum X_{max} to the antennas, which gives an estimate on the mass of the primary particle [11].

Another way for determining the mass of the primary cosmic ray has been developed at LOFAR [17]. For each event the arrival direction and energy are reconstructed from both LORA and radio-antenna array. A set of *ad-hoc* Monte Carlo simulations is then produced using these parameters. Results of simulations for pure protons and iron nuclei are compared with real data, and an estimate of X_{max} is obtained. This method allows to reconstruct X_{max} with an accuracy of 17 g/cm^2. Figure 4 shows the distribution of $< X_{max} >$ as function of the energy as obtained by applying the method here described (red points). Statistical uncertainties are indicated as black bars. Systematic uncertainties (shaded area) are also depicted and corresponds to $\sigma_{X_{max}} = {}^{+\,14}_{-\,10}$ g/cm^2 and to $\sigma_E = 27\%$. LOFAR measurements of the depth of the shower maximum are in agreement with previous results within statistical and systematic uncertainties [18].

5. Conclusions and outlook

All important results achieved by LOFAR in the past years have been reviewed in this article. The very dense area of antennas in the central part of the LOFAR array (six stations with 96 antennas each, spread over a circular area of roughly 320 m diameter) has allowed for a detail study of radio signals induced by cosmic rays in the atmosphere, and led to a deeper understanding of the radio emission processes. One of the current on-going research topics is focused on study the frequency spectrum of radio pulses and its sensitivity to properties of

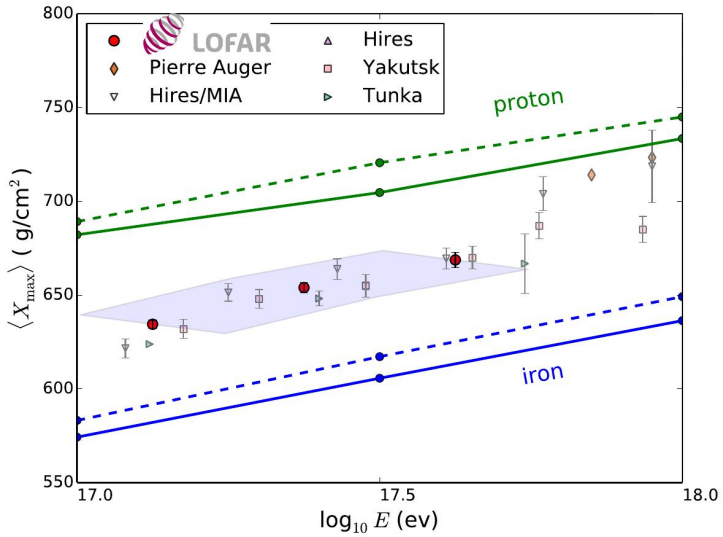

Figure 4. Distribution of the average depth of the shower maximum $< X_{\rm max} >$ as function of energy as obtained with the method described in [17]. LOFAR measurements (red points) are compared with results obtained by other experiments. Statistical uncertainties (black bars) are shown together with the systematic ones (shaded area). Simulation results obtained with QGSJETII.04 (solid lines) and EPOS-LHC (dashed lines) are also shown for showers initiated by protons (green lines) and iron nuclei (blue lines) [18].

primary cosmic rays. Simulations indicate that $X_{\rm max}$ determines the dependence of the frequency spectrum on the distance from the shower axis [19].

Other on-going researches regard the following aspects: to study the influence of atmospheric conditions on the radio emission, like air refractive index and humidity; to study in more detail atmospheric electric field during thunderstorm events; to study the possibility of triggering air showers only using radio antennas. The results presented here lead to a confirmation of the radio technique in detecting very high-energy cosmic rays.

References

[1] Jelley J V et al. 1965 *Nature* **205** 327–328
[2] Ardouin D et al. 2005 *Nucl. Instr. Meth. Phys. Res.* A **555** 148–163
[3] Falcke H et al. 2005 *Nature* **435** 313–316
[4] Van Haarlem M P et al. 2013 *A&A* **556** A2 53
[5] Nelles A et al. 2015 *JINST* **10** P11005
[6] Thoudam S et al. 2016 *Astropart. Phys.* **73** 34–43
[7] Thoudam S et al. 2014 *Nucl. Instr. Meth. Phys. Res.* A **767** 339
[8] Askaryan G A et al. 1962 *JETP* **14** 441–443
[9] Schellart P and Nelles A et al. 2013 *A&A* **560** A98
[10] Nelles A et al. 2014 *Astropart. Phys.* **60** 13–24
[11] Nelles A et al. 2015 *JCAP* **05** 018
[12] Nelles A et al. 2015 *Astropart. Phys.* **65** 11–21
[13] Schellart P et al. 2014 *JCAP* **10** 014
[14] Schellart P et al. 2015 *Phys. Rev. Lett.* **114** 165001
[15] Trinh T N G et al. *Phys. Rev.* D in press (arXiv:1511.03045)
[16] Corstanje A et al. 2014 *Astropart. Phys.* **61** 22–31
[17] Buitink S et al. 2014 *Phys. Rev.* D **90** 082003
[18] Buitink S et al. *Nature* in press
[19] Rossetto L et al. *Proc.* of the 34^{th} *Int. Cosmic Ray Conf.* PoS(ICRC2015)381 30 July–6 August, Den Haag